IEEE Access
Multidisciplinary : Rapid Review : Open Access Journal

Received January 7, 2020, accepted January 27, 2020, date of publication January 30, 2020, date of current version February 7, 2020.

Digital Object Identifier 10.1109/ACCESS.2020.2970493

Manipulator Trajectory Tracking of Fuzzy Control Based on Spatial Extended State Observer

CHUNGUANG FAN, ZONGWU XIE, YIWEI LIU, CHONGYANG LI, CHENGLONG YU, AND HONG LIU
State Key Laboratory of Robotics and System, Harbin Institute of Technology, Harbin 150001, China

Corresponding author: Zongwu Xie (xiezongwu@hit.edu.cn)

This work was supported in part by the National Key Research and Development Program of China under Grant 2017YFB1300400, in part by the National Natural Science Foundation of China under Grant 61503095, in part by the National Natural Science Foundation of China under Grant 91848202, and in part by the Foundation for Innovative Research Groups of the National Natural Science Foundation of China under Grant 51521003.

ABSTRACT This paper mainly studies the trajectory tracking control problem of the manipulator of TianGong-2 when capturing floating objects in the experimental cabin. Microgravity environment will lead to the existing control system of space robot can not produce good control effect. Different gravity environments change the design requirements of space robots, and the ground test cannot meet these space requirements. In this paper, a fuzzy control strategy based on a spatial extended state observer(FC-SESO) is proposed to solve these inconsistent problems. First, a spatial extended state observer is designed to estimate the influence of disturbance on the system. In order to estimate the disturbance quickly and accurately, a disturbance model including gust is established. Second, in order to ensure the rapid convergence of the desired trajectory, the fuzzy control law is derived. Based on Lyapunov stability theory, the stability of the control system based on the spatial extended state observer is proven. Finally, the proposed system is simulated and captured on the Tiangong-2 manipulator platform to verify the effectiveness of the control algorithm.

INDEX TERMS Fuzzy control, microgravity, spatial extended state observer, trajectory tracking control.

I. INTRODUCTION

Generally, the purpose of space robots is to assist astronauts in dangerous or repetitive work. At present, space robots have become an important part of maintaining the stable operation of the International Space Station, and they play vital roles in the on-orbit assembly and maintenance of space stations. Moreover, space robots are designed according to the processes of design with respect to assembly and debugging in the ground gravity environment, but in contrast, the actual use and service of these space robots are carried out in the space microgravity environment. Nevertheless, due to the change in the gravitational environment with respect to the aspects of both kinematics and dynamics, the robots tested in the ground gravitational environment can no longer meet the design requirements in the space microgravity environment. In fact, many scientists and scholars have developed strong interest in this issue. Thus far, many engineering experts have also developed various simulations and experimental methods for the microgravity environment [1]–[5]. Although these simulations and experimental strategies have eliminated the influence of gravity as much as possible, there still exist problems such as low fidelity, poor experimental precision or limited applicability: these problems can be solved only through simulation experiments in the microgravity environment. Taking this problem solution further, the difference between the simulation experiment and the real microgravity environment can only be addressed by experimenting in a microgravity environment. Fortunately, the author participated in the mechanical arm project of the TianGong-2 space station, which was designed by the research group, where the author applied the TianGong-2 humanoid mechanical arm system to complete the related experiments in orbit maintenance and on-orbit capture, and the experimental results fully verified the effectiveness of the proposed control method. Essentially, the operation of space robots is inseparable from the control system: therefore, at the beginning of the design of the controller, the difference in

The associate editor coordinating the review of this manuscript and approving it for publication was Xudong Zhao.

the control model caused by the change of the gravitational environment should be fully considered. Especially, with the vigorous development of the space industry, the task of space operation is becoming increasingly complicated, and hence, the required performance and accuracy of space robot systems are escalating. Therefore, a series of problems caused by changes in the gravitational environment should be given more consideration. At present, many experts and scholars have proposed numerous effective dynamic analysis methods and control algorithms for the trajectory tracking problem of space robots.

In the process of using manipulators to perform space tasks, many scholars have proposed effective solutions for different stages of the task [6]–[9]. Regarding the trajectory tracking control problem for multiple-degrees-of-freedom linear translation robot systems, literature [10] proposed a new model-free control law. Moreover, in literature [11], a dual-frame rigid-flexible trajectory control scheme based on virtual space aircraft is proposed. For the task of the space control strategy of the robot, literature [12] proposed a new local feedback method, which was adopted to introduce the feedback information into the local area. In addition, literature [13] proposed and studied the application of image-based visual service strategy in space mechanical arms. Furthermore, literature [14]–[16] studies the backstepping control problem of nonlinear systems and designed inversion controllers in different situations.

Most of the current researchers focus on the uncertainty of the model and the control of the capture task. Because there are fewer opportunities in the real on-orbit test, less research has been conducted on the controller with respect to the adaptive ability in response to model change. Therefore, this paper focuses on such research. The influence of the gravitational environment on the dynamic behavior of the space robot, through the design of the control scheme, solves the problem that the ground gravitational environment and the intermediate microgravity environment control effect are inconsistent.

The spacecraft's control characteristics in the microgravity environment are significantly different from those in the ground environment. Hence, how to design a proprietary controller for space robots in a microgravity environment based on these differences in the ground debugging phase has become a key research focus to solve this problem. Generally, the main problem encountered by space robots from design and commissioning to in-orbit service is that due to the difference between the ground environment and the space environment, it is impossible to establish a consistent control strategy, which leads to the result in which the designed effective controller of space robots tested in the ground environment cannot be directly applied for on-orbit operation in the space microgravity environment.

Although the observer technology has been widely used in manipulator control, most of the observers in this stage are based on linear models or linear systems [17], [18]. To estimate uncertain perturbations, many new methods are proposed for observer design [19]–[22]. By reducing the sensitivity of the controller to uncertainty, [23]–[27] propose solutions from different perspectives.

In terms of fuzzy control, many methods are designed to reduce the complexity of the system [28]–[35], and literature [36] proposed the dynamic feedback compensator to solve the asymptotic tracking problem. Literature [37] proposed an adaptive fuzzy sliding mode control (AFSMC) scheme. The chattering problem in tracking control is eliminated, and the steady-state error in tracking control is reduced. In literature [38], a nonsingular fast fuzzy terminal sliding mode controller (NFFTSMC) with interference estimator is designed to realize the convergence of finite time error and robust control.

Therefore, based on the specific problems and solutions of controller design in space microgravity environments, this paper realizes the consistency control strategy of ground maneuvering and on-orbit operation of space mechanical arm via designing a proprietary controller. From the perspective of interference suppression, the gusting of the air circulation system in the experimental cabin is regarded as a disturbance. Hence, an SESO is designed to estimate the disturbance, and then the FC-SESO is designed for the quick capture requirement: furthermore, we use the Lyapunov function to derive the proof of closed-loop stability. The simulation and experimentation of the task of catching floating balls in space are then carried out. The results show that the FC-SESO controller proposed in this paper exhibits good trajectory tracking performance for rapid capture tasks in different gravitational environments.

This paper is organized as follows. The second section analyzes the perturbation models under different conditions. To estimate perturbations, SESO is proposed in the third section. Based on the third section, the fourth section designs the fuzzy controller. The fifth section presents the simulation and experimentation of the proposed algorithm.

II. DYNAMIC MODEL UNDER DIFFERENT CONDITIONS

The main problem faced by space robots in the debugging process is the difference between the physical model and the actual environment. The controller designed for the debugging process cannot be directly used in the space environment, thus presenting difficulties for the debugging of the space robot on the ground, especially for completing the tasks of tracking, positioning, capturing and other control: more specifically, the spatial microgravity environment not only changes the gravitational load of the robot but also changes the other behaviors of the robot due to changes in gravitational load, along with the air circulation in the experimental cabin. However, the impact of the system requires a discussion of the kinetic models in different situations.

A. DYNAMIC MODEL IN THE GROUND GRAVITATIONAL ENVIRONMENT

The basic dynamic equation of the mechanical arm can be described as follows:

$$D(q)\ddot{q} + C(q, \dot{q})\dot{q} + G(q) = \tau \tag{1}$$

where, $D(q) \in R^{n\times n}$ is the matrix of system inertia, $C(q,\dot{q}) \in R^{n\times n}$ is the system's centrifugal force and Coriolis matrix, $G(q) \in R^n$ is the system gravitational load vector matrix, and $q = [q_1, q_2, \cdots, q_n]^T \in R^n$ is the displacement vector for the joint angle; moreover, $\tau = [\tau_1, \tau_2, \cdots, \tau_n]^T \in R^n$ is the driving torque for the joint of the mechanical arm.

Defining $x_1 = q$, $x_2 = \dot{q}$ and $x = [x_1^T, x_2^T]$, the system's state equation can be expressed as follows:

$$\begin{cases} \dot{x}_1 = x_2 \\ \dot{x}_2 = D^{-1}(x_1)(\tau - C(x_1, x_2)x_2 - G(x_1)) \end{cases} \tag{2}$$

The mechanical equation of the mechanical arm needs to meet the following characteristics:

Remark 1: $D(q)$ is symmetrically reversible and bounded.

Remark 2: When $k_b > 0, k_g > 0$ and positive definite functions $P(q,\dot{q})$ and $Q(q)$ exists, then:

$$\|G(q)\| \le k_g \|q\| \tag{3}$$
$$G^T(q)G(q) \le Q(q) \tag{4}$$
$$\|C(q,\dot{q})\| \le k_b \|\dot{q}\| \tag{5}$$
$$C^T(q,\dot{q})C(q,\dot{q}) \le P(q,\dot{q}) \tag{6}$$

Remark 3: When $\forall \eta \in R^n$, then $1/2\eta^T \dot{D}\eta = \eta^T C\eta$

Remark 4: When the given disturbance and error matrix satisfy $d_l \le \|d\| \le d_h$, $\delta D_l \le \|\delta D\| \le \delta D_h$, $\delta C_l \le \|\delta C\| \le \delta C_h$ and $\delta G_l \le \|\delta G\| \le \delta G_h$, then h and l are the upper and lower bound values, respectively.

B. DYNAMIC MODEL IN SPACE MICROGRAVITY

When the mechanical arm is in a spatial microgravity environment, its dynamic model is expressed as follows:

$$D_s(q_s)\ddot{q}_s + C_s(q_s,\dot{q}_s)\dot{q}_s = \tau_s \tag{7}$$

where, $D_s(q_s) \in R^{n\times n}$ is the inertia matrix, $C_s(q_s,\dot{q}_s) \in R^{n\times n}$ is the Coriolis force and centrifugal force vector, $q_s = [q_{1s}, q_{2s}, \cdots, q_{ns}]^T \in R^n$ is the displacement vector for the joint angle, and $\tau_s = [\tau_{1s}, \tau_{2s}, \cdots, \tau_{ns}]^T \in R^n$ is the driving torque for the joint of the mechanical arm.

When defining $x_{1s} = q_s$, $x_{2s} = \dot{q}_s$ and $x_s = [x_{1s}^T, x_{2s}^T]$, the system's state equation can then be expressed as follows:

$$\begin{cases} \dot{x}_{1s} = x_{2s} \\ \dot{x}_{2s} = D_s^{-1}(x_{1s})(\tau_s - C(x_{1s}, x_{2s})x_{2s}) \end{cases} \tag{8}$$

C. UNIFIED DYNAMIC MODEL OF MECHANICAL ARM

The control efficiency of equations (1) and (7) is effective only when the system parameters are accurately known. If there is any uncertainty in the model, the system will not be linearized, even if the model is accurate enough: the speed signal will contribute additional noise, makeing system linearization no longer reliable. Generally, it is difficult to produce an accurate model of the system in practical applications. There is always an existing modeling error, which can be considered as an internal disturbance, recorded as τ_i. In addition, changes caused by changes in gravity in a microgravity environment, such as friction and load changes, are called external disturbances, which are recorded as τ_o. Finally, the disturbance caused by the change of airflow in the experimental cabin to the robot arm is called random disturbance, which is recorded as τ_r. Considering these disturbances, the spatial mechanical arm system dynamics model can be described in the following form:

$$D_0(q)\ddot{q} + C_0(q,\dot{q})\dot{q} + G_0(q) = \tau + \tau_d \tag{9}$$
$$\tau_d = \tau_i + \tau_o + \tau_r \tag{10}$$

Here, τ_d refers to the sum of all disturbances and is an unknown time-varying disturbance.

$$D_0(q) = D(q) - \delta D(q) \tag{11}$$
$$C_0(q,\dot{q}) = C(q,\dot{q}) - \delta C(q,\dot{q}) \tag{12}$$
$$G_0(q) = G(q) - \delta G(q) \tag{13}$$

where, $D_0(q), C_0(q,q), G_0(q)$ is the nominal value of the model, meantime, $\delta D(q), \delta C(q,q), \delta G(q)$, respectively, refer to the system inertia matrix, the centrifugal force and the Coriolis force matrix, and the error matrix of the gravitational load vector matrix.

When defining $x_{1r} = q, x_{2r} = \dot{q}, x_r = [x_{1r}^T, x_{2r}^T]^T$, the state equation of the system can be expressed as follows:

$$\begin{cases} \dot{x}_{1r} = x_{2r} \\ \dot{x}_{2r} = D_0{}^{-1}(x_{1r})(\tau + \tau_d - C_0(x_{1r}, x_{2r})x_{2r} - G_0(x_{1r})) \end{cases} \tag{14}$$

Therefore, it is necessary to design a control strategy that can compensate the adaptive dynamic characteristics in different gravitational environments without changing the controller structure and controller parameters.

D. DISTURBANCE MODEL

1) WIND GUST MODEL

Due to the experimental cabin in which the mechanical arm is located being within the space environment, there is no natural convection of air in the sealed cabin, furthermore, the establishment of the manned environment needs to be ensured by forced ventilation in the cabin through the ventilation system, which leads to flotation in the cabin and the situation in which the inner ball moves with the air flow field and also interferes with the mechanical arm. Therefore, this scene can be approximated as a miniature wind field model.

The wind field model used in this section primarily consists of two parts: a static dominant wind direction strength model and gust model based on standard power spectral density (PSD) [39]. The static component characterizing the basic dominant wind characteristics can be initialized by the upstream wind supply system, and the gust model of the PSD is derived from the Dryden [40] model, which relies on the static wind model to generate the necessary parameters for the PSD.

$$v_w(z) = \frac{1}{k} v_w^* \ln\left(\frac{z}{z_0}\right) \tag{15}$$

Here z is the height of the ball above the ground of the experimental cabin, z_0 is the length in the experimental cabin,

k is the von Kaman constant, and v_w^* is the friction speed between the air and the ground of the experimental cabin. $v_w(z)$ is the wind speed at height, which can be simplified to the typical value of open terrain [41], therefore, when given $v_w(z)$ and z, v_w^* can be solved by equation (15). Additionally, the upper bound value can be expressed as follows:

$$\bar{z} = b\frac{v_\omega^*}{2\omega_e \sin\phi_l} \tag{16}$$

where, b is a scale constant, ϕ is the earth's latitude at a given location, and ω_e is the angular velocity of the earth on the north-south axis, the first two equations are used to determine the average wind speed at a given height in the surface boundary layer. The Dryden gust model is defined as the sum of the sinusoidal excitations, and is expressed in the following form:

$$\upsilon_\omega(t) = \upsilon_\omega^0 + \sum_{i=1}^{n} a_i \sin(\Omega_i t + \varphi_i) \tag{17}$$

In the formula, $\upsilon_\omega(t)$ is the time-dependence estimation value of the given time t's wind vector, Ω_i, φ_i is the randomly selected frequency and phase shift, n is the sine, a_i is the amplitude of the sine, and υ_ω^0 is the ambient wind vector (or static wind vector), thus, the amplitude of a_i can be given by the following:

$$a_i = \sqrt{\Delta\Omega_i \Phi(\Omega_i)} \tag{18}$$

In the formula, $\Delta\Omega_i$ refers to the interval between frequency and $\Phi(\Omega_i)$, the power spectral densities between vertical wind and horizontal wind of PSD are different and can be derived from the following equation:

$$\Phi_h(\Omega) = \sigma_h^2 \frac{2L_h}{\pi} \frac{1}{1 + (L_h\Omega)^2} \tag{19}$$

$$\Phi_\upsilon(\Omega) = \sigma_\upsilon^2 \frac{L_\upsilon}{\pi} \frac{1+3(L_\upsilon\Omega)^2}{(1 + (L_h\Omega)^2)^2} \tag{20}$$

In these equations, σ_h and σ_υ represent the horizontal and vertical turbulence intensity, respectively, while L_h and L_υ represent horizontal and vertical gust length scales. Therefore, the wind field model defines the wind speed at a given altitude and varies with respect to time and altitude.

2) WIND GUST DISTURBANCE

According to the Dryden gust model, we assume that the disturbance caused by the wind field is proportional to the wind speed, so d_ω can be described based on stochastic theory [42], furthermore, it can be defined as the sum of sinusoidal excitations [43]

$$d_{w,k}(t) = d_{w.k}^0 + \sum_{i=1}^{n_k} a_{k,i} \sin(\varpi_{k,i} t + \varphi_{k,i}) \tag{21}$$

In the formula, $d_{w,k}(t)$ is the time-varying description of wind disturbances during the cycle for the given time t. $\varpi_{k,i}$, $\varphi_{k,i}$ represents the randomly selected frequency and phase shif, n_k is sine, $a_{k,i}$ is a sinusoidal amplitude, and $d_{w.k}^0$ is a static wind disturbance. Therefore, in general, the disturbance caused by the ventilation system of the robot arm is high-order and non-Gaussian and exhibits strong randomness and nonlinearity.

III. DESIGN OF SPATIAL EXTENDED STATE OBSERVER

The spatial extended state observer is actually a state observer, which can not only reproduce the state quantity of the control object but also estimate the ‘‘extended state’’ of the uncertainty factor of the control object model and the real-time value of the interference. This observer is particularly suitable for the estimation of slow aperiodic disturbances.

A. GENERAL FORM OF SPATIAL EXTENDED STATE OBSERVER

The uncertain nonlinear system subjected to external disturbances can be expressed by equation(22):

$$x^{(n)} = f(x, \dot{x}, \ldots, x^{(n-1)}, t) + \omega(t) + bu(t) \tag{22}$$

In the formula, $f(x, \dot{x}, \ldots, x^{(n-1)}, t)$ is a nonlinear unknown function that is composed of various state variables of the system.

$w(t)$ is an unknown external disturbance of the system;

$u(t)$ is a control variable, $x(t), \dot{x}(t), \ldots x^{(n-1)}(t)$ is the state variable of the system, and $x(t)$ is direct-measurable or indirect-measurable, and thus, the system $x_1 = x(t), x_2 = \dot{x}(t), \ldots, x_n = x^{(n-1)}(t)$ can be rewritten as follows:

$$\begin{cases} \dot{x}_1 = x_2 \\ \dot{x}_2 = x_3 \\ \quad \vdots \\ \dot{x}_n = f(x_1, x_2, \ldots, x_n) + w(t) + bu(t) \end{cases} \tag{23}$$

Then, a nonlinear system can be constructed:

$$\begin{cases} \dot{z}_1 = z_2 - g_1(z_1 - x(t)) \\ \dot{z}_2 = z_3 - g_2(z_1 - x(t)) \\ \quad \vdots \\ \dot{z}_n = z_{n+1} - g_n(z_1 - x(t)) + bu(t) \\ \dot{z}_{n+1} = -g_{n+1}(z_1 - x(t)) \end{cases} \tag{24}$$

We assume that $a(t) = f(x, \dot{x}, \ldots, x^{(n-1)}, t) + w(t)$, as long as the nonlinear function $g_1(z), g_2(z), \ldots, g_{n+1}(z)$ is properly selected, to track each state variable of the system (22) and $a(t)$ by each state variable of the system (24) for which input is $x(t)$, and then obtain the state observer which is engaged with a n-order nonlinear system. Because $a(t)$ contains the uncertain objects and external disturbances of the system (22), therefore, it can be compensated accordingly in the control operation so that the control system shall be endowed with strong adaptability.

B. DESIGN OF SPATIAL EXTENDED STATE OBSERVER

To eliminate the influence of the overall disturbance of the previous analysis on the control performance of the system,

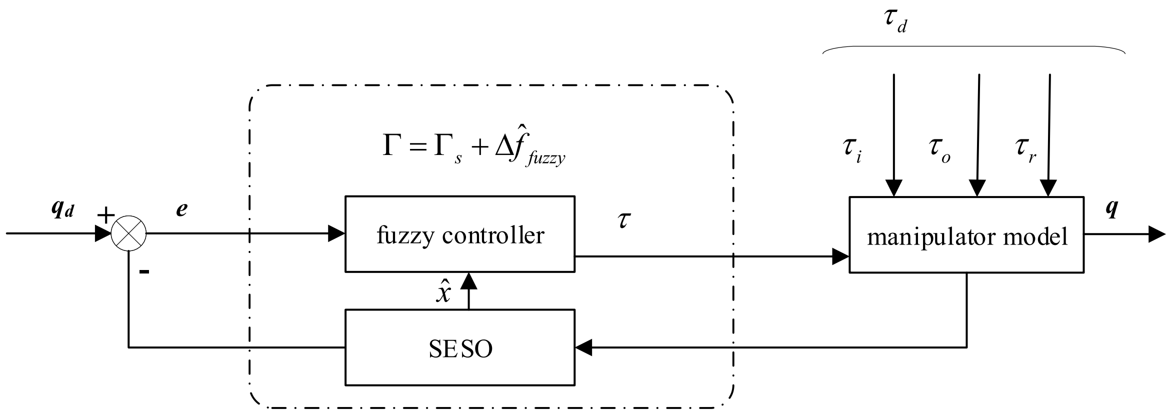

FIGURE 1. Diagram of an FC-SESO controller.

this chapter regards the dynamic parameters caused by the microgravity environment, the disturbance caused by the friction model change, and the external disturbance caused by the ventilation system in the space mechanical arm system as the general disturbance. Via the related assessment of this general disturbance, conducted by designing the extended state observer, along with its further fuzzy controller design, the general disturbance can be restrained. To design the extended state observer and to extend the general disturbance of the space mechanical arm system to be a new state variable of the system, defined as $x_3 = \tau_d = \tau_i + \tau_o + \tau_r$, the state variable of the system therefore becomes $x = [x_1, x_2, x_3]$, assuming that $h(t)$ represents the differential of x_3, and then, the system equation becomes the following:

$$\begin{cases} \dot{x}_1 = x_2 \\ \dot{x}_2 = D_0{}^{-1}(x_1)\tau - D_0{}^{-1}(x_{1r})C_0(x_1, x_2)x_2 + x_3 \\ \dot{x}_3 = h(t) \end{cases} \tag{25}$$

Since the space mechanical arm is a typical nonlinear system, parameter uncertainties exist. Moreover, the external disturbances such as nonlinear friction and gust model are also present, which reduce the dynamic performance of the system control; therefore, to improve the control precision of the space mechanical arm system, it is necessary to improve the control accuracy of the space mechanical arm system and thus to eliminate the effects of disturbances on the system. To achieve this goal, this paper designs an extended state observer to observe the state of the system and the overall disturbance. For the sake of convenience in designing the extended state observer, both general disturbance x_3 and its related derivative $h(t)$ are assumed to be bounded.

For the extended system (25), since the observable matrix is a full rank matrix, the system (25) is observable according to literature [44], and the spatial extended state observer is designated as follows:

$$\begin{cases} \dot{\hat{x}}_1 = \hat{x}_2 + g_1(x_1 - \hat{x}_1) \\ \dot{\hat{x}}_2 = \hat{x}_3 + g_2(x_1 - \hat{x}_1) \\ \vdots \\ \dot{\hat{x}}_n = \hat{x}_{n+1} + g_n(x_1 - \hat{x}_1) + bu \\ \dot{\hat{x}}_{n+1} = g_{n+1}(x_1 - \hat{x}_1) + h(\hat{x}, \omega) \end{cases} \tag{26}$$

where $\hat{x} = \left[\hat{x}_1, \hat{x}_2, \cdots, \hat{x}_{n+1}\right]^T \in R^{n+1}$ and observer gain is defined as $g_i = [g_1, g_2, \cdots, g_{n+1}] = \left[\omega_0\alpha_1, \omega_0^2\alpha_2, \cdots, \omega_0^{n+1}\alpha_{n+1}\right]$ where α_i satisfies the characteristic polynomial equation $s^{n+1} + \alpha_1 s^n + \cdots + \alpha_n s + \alpha_{n+1} = (s+1)^{n+1}$ where $\alpha_i = (n+1)!/i!(n+1-i)!$, $\omega_0 > 0$ The observer estimation error can be shown as

$$\begin{cases} \dot{\tilde{x}}_1 = \tilde{x}_2 - \omega_0\alpha_1\tilde{x}_1 \\ \dot{\tilde{x}}_2 = \tilde{x}_3 - \omega_0^2\alpha_2\tilde{x}_1 \\ \vdots \\ \dot{\tilde{x}}_n = \tilde{x}_{n+1} - \omega_0^n\alpha_n\tilde{x}_1 \\ \dot{\tilde{x}}_{n+1} = h(x, \omega) - h(\hat{x}, \omega) - \omega_0^{n+1}\alpha_{n+1}\tilde{x}_1 \end{cases} \tag{27}$$

when $n = 3$

$$\begin{cases} \dot{\hat{x}}_1 = \hat{x}_2 - 3\omega_0(\hat{x}_1 - x_1) \\ \dot{\hat{x}}_2 = D_0{}^{-1}(x_1)\tau - D_0{}^{-1}(x_{1r})C_0(x_1, x_2)x_2 \\ \qquad + \hat{x}_3 - 3\omega_0^2(\hat{x}_1 - x_1) \\ \dot{\hat{x}}_3 = -\omega_0^3(\hat{x}_1 - x_1) \end{cases} \tag{28}$$

Here, $\hat{x} = [\hat{x}_1, \hat{x}_2, \hat{x}_3]^T$ is the state of observation, and $\omega_0 > 0$ is the observer gain.

Defining observation error $\tilde{x}_i = x_i - \hat{x}_i, i = 1, 2, 3$ according to formulas (25) and (28), it would transform into the following:

$$\begin{cases} \tilde{x}_1 = \tilde{x}_2 - 3\omega_0\tilde{x}_1 \\ \tilde{x}_2 = \tilde{x}_3 - 3\omega_0^2\tilde{x}_1 \\ \tilde{x}_3 = h(t) - \omega_0^3\tilde{x}_1 \end{cases} \tag{29}$$

In equation (29), the transfer function of general dynamics $h(t)$ and observation error $\tilde{x}$ is

$$\frac{\tilde{x}_1}{h} = \frac{1}{s^3 + 3\omega_0 s^2 + 3\omega_0^2 s + \omega_0^3} \tag{30}$$

Therefore, the characteristic polynomial of equation (29) can be written as follows:

$$\lambda_0(s) = (s + \omega x_0)^3 \tag{31}$$

As can be seen from the above equation, the observer gain ω_0 is determined by the bandwidth of the system. Thus, in the process of selecting the gain ω_0, the factors of both observation performance and robustness of the observer shall be seriously considered.

C. CONVERGENCE PROOF OF THE SPATIAL EXTENDED STATE OBSERVER

To prove the convergence of the extended observer (26), defining $\varepsilon_i = \tilde{x}_i \Big/ \omega_0^{i-1}, i = 1, 2, 3$, the formula (29) can be expressed in the following form:

$$\dot{\varepsilon} = \omega_0 A \varepsilon + M \frac{h(x, \omega)}{\omega_0^2} \tag{32}$$

where A is Hurwitz, $M = [0, 0, 1]^T$, and the following lemma can then be obtained:

Lemma 1: assumes that extended state $h(t)$ is bounded, the observing state $\hat{x}_i, i = 1, 2, 3$ is bounded and has a constant $\sigma_i > 0$ greater than zero, and the finite time constant $T > 0$, which thus enables the following formula fitting; moreover, c is the corrected integer.

$$|\tilde{x}_i| \le \sigma_i, \quad \sigma_i = O\left(\frac{1}{\omega_0^c}\right); \; i = 1, 2, 3, \; \forall t \ge T \tag{33}$$

Proof: For the proof process, please refer to literature [44] ■

Remark 5: according to lemma 1 and literature [44], it can be determined that the extended state observer (26) is stable, and the observation error can be adjusted by adjusting the bandwidth parameter to any small value. By choosing a larger observer gain, the observed performance can be effectively improved. Nevertheless, the consequences of doing so can weaken the observer's robustness and cause high frequency vibrations. Therefore, it is necessary to select an appropriate observer gain in combination with robustness requirements and system observation performance.

Figure 2 shows the estimated error curves under different bandwidths, where (a) represents the estimation error under the ground gravitational environment, and (b) represents the estimation error under the space microgravity environment. It can be seen from the figure that the perturbation estimation error decreases with the increase in bandwidth. The relationship between tracking error and bandwidth is further explained.

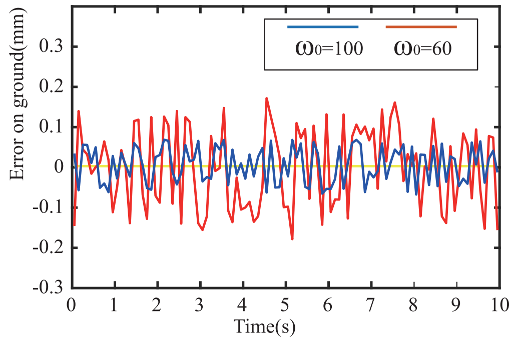

(a) Estimated error on ground

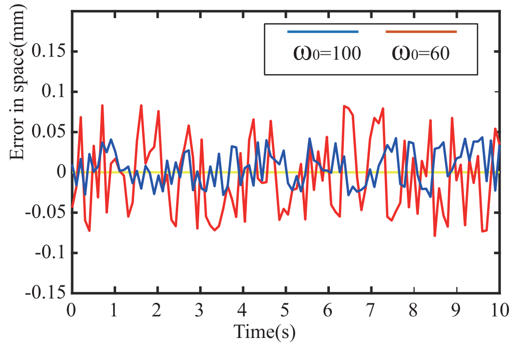

(b) Estimated error in space

FIGURE 2. Estimated error of proposed method with different design parameters.

IV. FUZZY CONTROL BASED ON SPATIAL EXTENDED STATE OBSERVER

A. EXPRESSIVE METHOD OF FUZZY CONTROLLER

It is assumed that the fuzzy algorithm is the mapping from $U \subseteq R^n$ to R, and the fuzzy knowledge base is a collection of IF-THEN rules that contain the following forms:

R(j): IF x_1 is F_l^j and x_2 is F_2^j and x_n is F_n^j
THEN y_f^j is $C^j (j = 1, 2, \ldots, m)$

Here, $x_f = [x_1, x_2, \cdots x_n]^T \in U$ is the input to the fuzzy logic system, $y_f \in R$ is the output of the fuzzy logic system, F_n^j is the fuzzy set of inputs, C^j is the fuzzy set of the output, and by applying the univariate fuzzification, fuzzy inference engine and central average defuzzification, the output value of the fuzzy system can be expressed as follows:

$$y_f(x_f) = \frac{\sum_{j=1}^{m} \bar{y}_f^j \left(\prod_{i=1}^{n} \mu_{F_j^i}(x_i)\right)}{\sum_{j=1}^{m} \left(\prod_{i=1}^{n} \mu_{F_j^i}(x_i)\right)} \tag{34}$$

Among them, $\bar{y}_f^j = \max \mu_{C^j}(y_f^j), \mu_{C^j}(\bar{y}_f^j) = 1$ and $\mu_{F_j^i}$ is the membership function of the input, and μ_{C^j} is the membership function of the output; thus, the fuzzy basis function is defined as follows:

$$\xi_j(x_f) = \frac{\prod_{i=1}^{n} \mu F_i^j(x_i)}{\sum_{j=1}^{m} \left(\prod_{i=1}^{n} \mu F_i^j(x_i)\right)} \tag{35}$$

The fuzzy system can then be rewritten as follows:

$$y_f(x_f) = \xi^T(x_f)\theta \tag{36}$$

where $\xi(x_f) = [\xi_1(x_f), \xi_2(x_f), \ldots, \xi_m(x_f)]^T$ is the regression vector, and $\theta = [\bar{y}_f^1, \bar{y}_f^2, \ldots, \bar{y}_f^m]^T$ is the parameter vector of the fuzzy system.

B. FUZZY CONTROLLER DESIGN

This paper uses the fuzzy system to approximate unknown nonlinear functions $u_i(x)$ and $w_{ij}(x)(i = 1, 2, \ldots, n; j = 1, 2, \ldots, n)$ to design automatically adaptive control laws.

The auxiliary variables are constructed as follows:

$$z_1 = x_1 - x_{1d} = q - q_d \tag{37}$$

Select virtual control quantity

$$\alpha_1 = \lambda z_1 \tag{38}$$

Define

$$z_2 = x_2 - x_{2d} + \alpha_1 \tag{39}$$

Select virtual control quantity

$$\alpha_2 = D_0 \ddot{q}_s + C_0 \dot{q}_s - \eta z_2 - \beta z_1 \tag{40}$$

Here, $D_0(q), C_0(q, \dot{q})$ represents the nominal part of the model in a gravitational environment, η, β, λ is a positive definite diagonal coefficient matrix, and $\dot{q}_s = x_{2d} - \alpha_1$, $\ddot{q}_s = \dot{x}_{2d} - \dot{\alpha}_1$.

The system control input can be expressed as follows:

$$\tau = \alpha_2 - \Gamma_{fuzzy} \tag{41}$$

where $\Gamma_{fuzzy} = \Gamma_s + \Delta\hat{f}_{fuzzy}$ is a fuzzy compensation controller, $\Gamma_s = ksgn(z_2)$, and $k \in R^{n\times n}$ is a positive definite diagonal coefficient matrix.

Setting $\Delta\hat{f}_{fuzzy} = [\Delta\hat{f}_{fuzzy1}, \Delta\hat{f}_{fuzzy2}, \ldots, \Delta\hat{f}_{fuzzyi}], i = 1, 2, \ldots, n$ as the estimated value of Δf and the output of the fuzzy control system, then setting the auxiliary variable z_2 as input to the fuzzy logic control system, and respectively dividing the input variables and output variables into 7 fuzzy sets

$$\{NB, NM, NS, ZO, PS, PM, PB\},$$

the following membership function is defined:

Fuzzy sets and fuzzy rules are defined as follows:

(1) If z_{2i} is PB then $\Delta\hat{f}_{fuzzy}$ is PB

(2) If z_{2i} is PM then $\Delta\hat{f}_{fuzzy}$ is PM

(3) If z_{2i} is PS then $\Delta\hat{f}_{fuzzy}$ is PS

(4) If z_{2i} is ZO then $\Delta\hat{f}_{fuzzy}$ is ZO

(5) If z_{2i} is NS then $\Delta\hat{f}_{fuzzy}$ is NS

(6) If z_{2i} is NM then $\Delta\hat{f}_{fuzzy}$ is NM

(7) If z_{2i} is NB then $\Delta\hat{f}_{fuzzy}$ is NB

In the fuzzy controller, the range of input parameters is set to $[-pi, pi]$, the range of output parameters is set to $[-2, 2]$, input and output variables are decomposed into seven fuzzy zones, and the membership function is shown in Figure 3.

$$\mu_A(x_i) = \exp\left[-(\frac{x_i - \alpha_i}{\sigma})^2\right] \tag{42}$$

The output of the fuzzy controller is then

$$\Delta\hat{f}_{fuzzyi} = \frac{\sum_{m=1}^{M} \theta_{fi}^m \mu A^{m(s_i)}}{\sum_{m=1}^{M} \mu A^{m(s_i)}} = \theta_{fi}^T \psi_{fi}(z_{2i}) \tag{43}$$

In the formula,

$$\psi_{fi}(z_{2i}) = \left[\psi_{fi}^1(z_{2i}), \psi_{fi}^2(z_{2i}), \ldots, \psi_{fi}^M(z_{2i})\right]^T$$

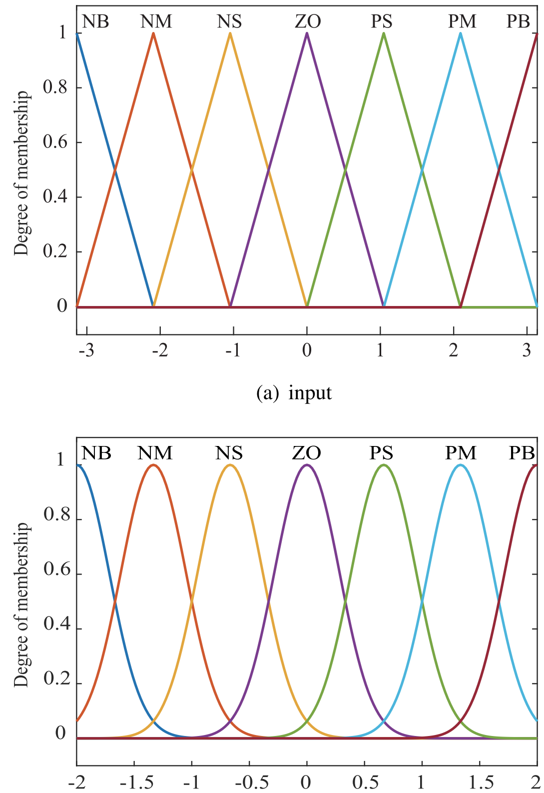

(a) input

(b) output

FIGURE 3. Membership functions of input and output variables.

$$\theta_{fi} = \left[\theta_{fi}^1, \theta_{fi}^2, \ldots, \theta_{fi}^M\right]^T$$

$$\psi^m(x) = \prod_{i=1}^{n} \mu A_i^m(x_i^*) \Bigg/ \sum_{m=1}^{M} \prod_{i=1}^{n} \mu A_i^m(x_i^*)$$

Assuming that Δf_{fuzzy}^* is the ideally optimal estimation of Δf_{fuzzy} and supposing that $w_i = \Delta f_{fuzzyi} - \Delta f_{fuzzyi}^*$, according to the universal approximation ability of the fuzzy system, the following can be verified:

$$\left|\Delta f_{fuzzyi} - \Delta f_{fuzzyi}^*\right| \le \bar{w}_i, \quad \bar{w}_i > 0 \tag{44}$$

In the formula, $\Delta f_{fuzzyi}^* = \theta_{f_i^*}^T \psi_{f_i^*}(z_{2i})$.

We define

$$\begin{aligned}\Delta\tilde{f} &= \Delta f_{fuzzy}^* - \Delta\hat{f}_{fuzzy} \\ &= \left[\Delta\tilde{f}_1, \Delta\tilde{f}_2, \ldots, \Delta\tilde{f}_i\right]\end{aligned} \tag{45}$$

In the formula, $\Delta\tilde{f} = \tilde{\theta}_{fi}^T \psi_{fi}(z_{2i}), \tilde{\theta}_{fi} = \hat{\theta}_{fi} - \theta_{f_i^*}$.

Then, there is

$$\Delta f_{fuzzyi} - \Delta\hat{f}_{fuzzyi} = \Delta\tilde{f}_i + w_i \tag{46}$$

The automatically adaptive law in designing $\hat{\theta}_{fi}$ is as follows:

$$\dot{\hat{\theta}}_{fi} = z_{2i}\psi_{fi}(z_{2i}) \tag{47}$$

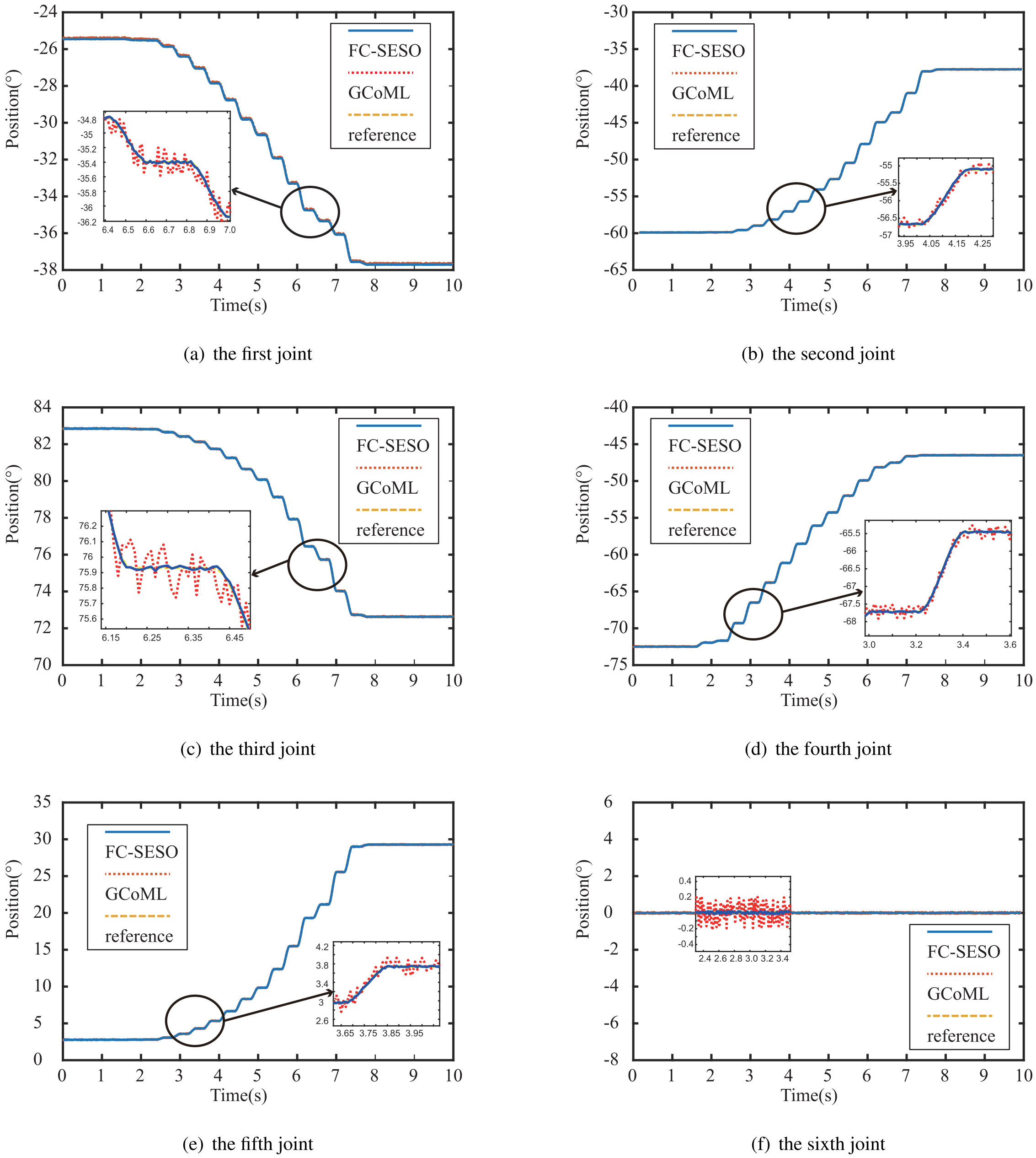

(a) the first joint

(b) the second joint

(c) the third joint

(d) the fourth joint

(e) the fifth joint

(f) the sixth joint

FIGURE 4. **Ground environment simulation experiment.**

The control input for the system is obtained as follows:

$$\tau = D_0 q_s + C_0 q_s - \alpha z_2 - \beta z_1 - \Gamma_{fuzzy} \tag{48}$$

Among them, α, β is the matrix of positive definite diagonal coefficients.

C. STABILITY PROOF OF FUZZY CONTROLLER

The Lyapunov function is taken as follows:

$$V_1 = \frac{1}{2} z_1^T \beta z_1 \tag{49}$$

The derivation of the above formula can be obtained as follows:

$$\dot{V}_1 = z_1^T \beta z_2 - \lambda z_1^T \beta z_1 \tag{50}$$

The Lyapunov function of the subsystem can be taken as follows:

$$V_2 = V_1 + \frac{1}{2} z_2^T D_0 z_2 \tag{51}$$

The derivation of the above formula can be obtained as follows:

$$\dot{V}_2 = \beta z_1^T z_2 + z_2^T D_0 \dot{z}_2 + \frac{1}{2} z_2^T \dot{D}_0 z_2 \tag{52}$$

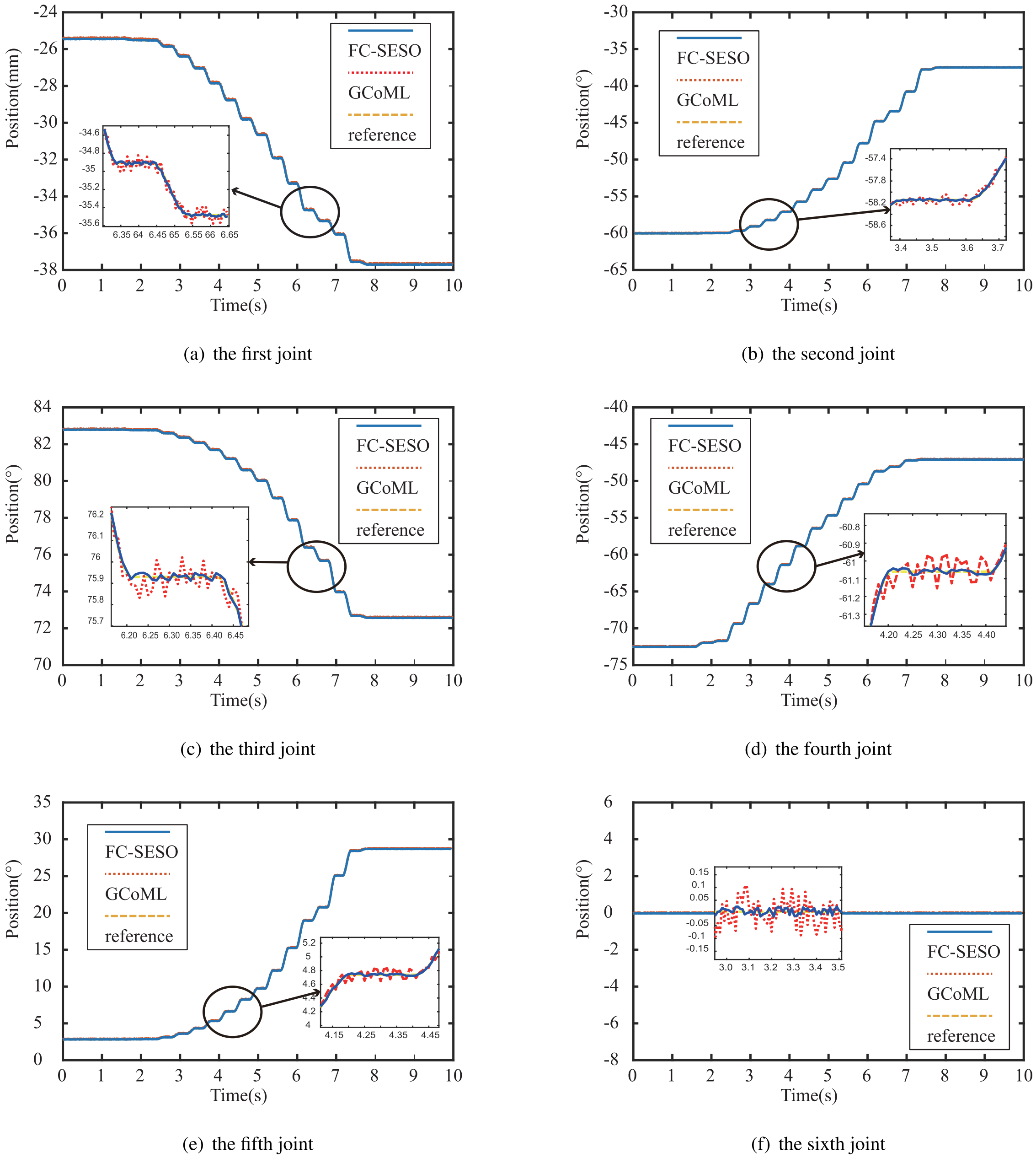

(a) the first joint

(b) the second joint

(c) the third joint

(d) the fourth joint

(e) the fifth joint

(f) the sixth joint

FIGURE 5. Space environment simulation experiment.

To simplify the representation, replace the above symbols with the following:

$$\Delta f = \delta D(q)\ddot{q} + \delta C(q,\dot{q})\dot{q} - \tau_d \tag{53}$$

Thus, $\dot{V}_2$ can be expressed as follows:

$$\dot{V}_2 = \sum_{i=1}^{n} (z_{2i}(\Delta f_i - k_i)) - z_2^T \eta z_2 \tag{54}$$

The Lyapunov function of the system is defined as follows:

$$V = V_2 + \frac{1}{2}\sum_{i=1}^{n} (\tilde{\theta}_{f_i}^T \tilde{\theta}_{f_i}) \tag{55}$$

The V derivation can be obtained as follows:

$$\begin{aligned}\dot{V} &= \dot{V}_2 + \frac{1}{2}\sum_{i=1}^{n} (\dot{\theta}_{f_i}^T \tilde{\theta}_{f_i} + \tilde{\theta}_{f_i}^T \dot{\theta}_{f_i}) \\ &\leq \sum_{i=1}^{n} z_{2i}\Big[\Delta f_i - k_{ii} sgn(z_{2i}) \\ &\quad - (\theta_{f_i^*}^T \psi_{f_i^*}(z_{2i}) - \tilde{\theta}_{f_i}^T \psi_{f_i}(z_{2i}))\Big] \\ &\quad + \sum_{i=1}^{n} \tilde{\theta}_{f_i}^T \dot{\theta}_{f_i}^T - z_2^T \eta z_2\end{aligned}$$

$$
\begin{aligned}
&\leq \sum_{i=1}^{n} z_{2i}\left[\Delta f_i - k_{ii}sgn(z_{2i}) - \theta_{f_i^*}^{T}\psi_{f_i^*}(z_{2i})\right] \\
&\quad + \sum_{i=1}^{n} \tilde{\theta}_{f_i}^{T}\left(z_{2i}\psi_{f_i}(z_{2i}) + \dot{\tilde{\theta}}_{f_i}^{T}\right) - z_2^T\eta z_2 \\
&\leq \sum_{i=1}^{n} z_{2i}\left[\bar{w}_i - k_{ii}sgn(z_{2i})\right] \\
&\leq \sum_{i=1}^{n} \left[(\bar{w}_i - k_{ii})\left|z_{2i}\right|\right] - z_2^T\eta z_2 \qquad (56)
\end{aligned}
$$

If there is a small positive real number γ_i, then

$$
\left|\Delta f_{fuzzy} - \theta_{f_i^*}^{T}\psi_{f_i}(z_{2i})\right| \leq w_i \leq \gamma_i\left|z_{2i}\right|, \quad 0 \leq \gamma_i \leq 1
$$

can be obtained, further leading to

$$
z_{2i}\left|\Delta f_i - \theta_{f_{id}}^{T}\psi_{f_i}(z_{2i})\right| \leq \gamma_i|z_{2i}|^2 = \gamma_i {z_{2i}}^2
$$

and hence, equation (56) can be further organized as follows:

$$
\dot{V} \leq \sum_{i=1}^{n}\gamma_i z_{2i}^2 - z_2^T\eta z_2 \leq \sum_{i=1}^{n}(\gamma_i - \eta_i)z_{2i}^2 \qquad (57)
$$

Thus, if and only if $z_2 = 0$, $\dot{V} = 0$, then the closed-loop system becomes progressively stable.

V. SIMULATION AND EXPERIMENTAL RESULTS

The simulation and experimental platform adopts the TianGong-2 manipulator system [45], where the parameters of the controller and observer are shown as follows:

$$
\eta = \beta = \begin{bmatrix} 5 & 0 & 0 & 0 & 0 & 0 \\ 0 & 5 & 0 & 0 & 0 & 0 \\ 0 & 0 & 5 & 0 & 0 & 0 \\ 0 & 0 & 0 & 5 & 0 & 0 \\ 0 & 0 & 0 & 0 & 5 & 0 \\ 0 & 0 & 0 & 0 & 0 & 5 \end{bmatrix}
$$

$$
k = \begin{bmatrix} 30 & 0 & 0 & 0 & 0 & 0 \\ 0 & 30 & 0 & 0 & 0 & 0 \\ 0 & 0 & 30 & 0 & 0 & 0 \\ 0 & 0 & 0 & 30 & 0 & 0 \\ 0 & 0 & 0 & 0 & 30 & 0 \\ 0 & 0 & 0 & 0 & 0 & 30 \end{bmatrix}
$$

$$
\lambda = I_6 \times 10^2, \quad \omega_0 = 60(100)
$$

A. SIMULATION RESULTS

To verify the effectiveness of the control strategy designed in this paper, simulation research on the trajectory tracking control of the mechanical arm in the ground gravity environment and the space microgravity environment is carried out by the author. The controller block diagram is shown in Figure 1.

It can be determined from the simulation results that the controller designed in this paper can achieve good control of the dynamic unified model under different gravitational environments, without changing the control parameters or controller structure, in terms of effectively solving the proposed control problem. The control scheme in this paper is compared with the control scheme in literature [46], which adopts a gravity compensation calibration method based on model learning (GCoML). According to the structure of the connecting rod and the sampled data, the regression matrix equation is established. Least squares regression and L2 norm regularization are used to find the optimal solution, and the gravity compensation model of the robot arm is updated in real time. This is a simple, effective and novel control method in the engineering field.

The ground gravity environment simulation is shown in Figure 4, and the space microgravity environment simulation is shown in Figure 5, proving the superiority of the control method proposed in this paper.

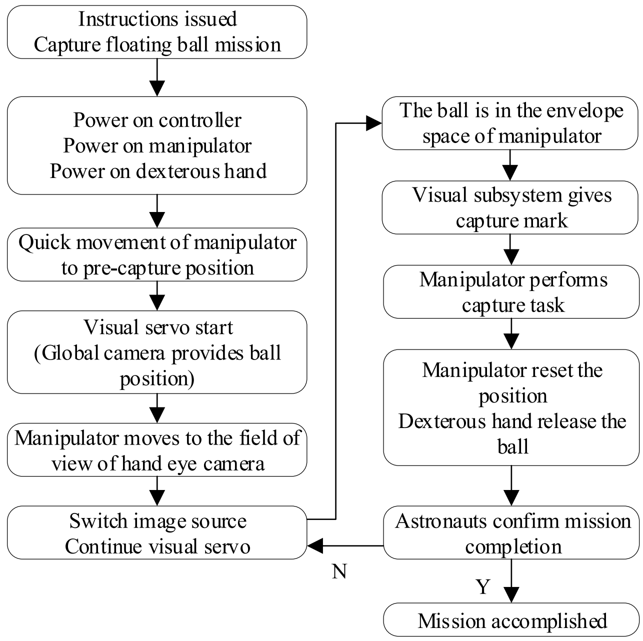

FIGURE 6. Capture experimental flow chart.

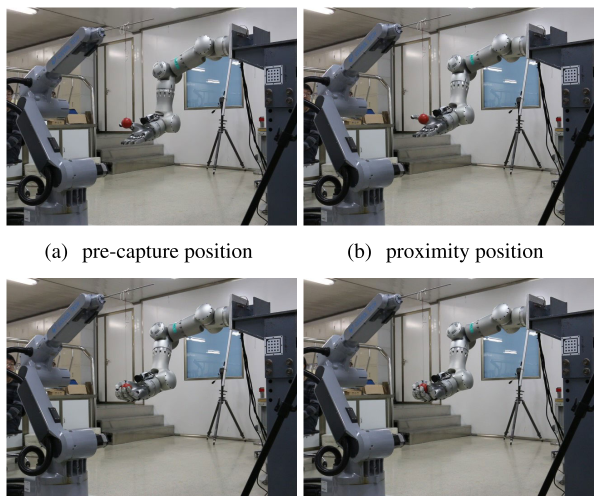

(a) pre-capture position (b) proximity position

(c) capture position (d) implementation of capture

FIGURE 7. Ground experiment of the capture mission.

(a) pre-capture position

(b) proximity position

(c) capture position

(d) implementation of capture

FIGURE 8. Space experiment of the capture mission.

The simulation results show that the proposed method offers higher tracking accuracy and better performance in chattering suppression.

B. EXPERIMENTAL RESULTS

The experimental flow of the capture task is shown in Figure 6, and the ground experiment is shown in Figure 7. In the ground experiment, to simulate the floating state of the small ball in the space microgravity environment, the off-line programming of the industrial robot is used to guide the small ball. The space experiment is shown in Figure 8. In the space experiment, the astronauts release the small ball in the cabin space, and the small ball floats freely in space. Finally, the mechanical arm system is used to catch the small ball. By using the control method proposed in this paper, the experiments of ground gravity and space microgravity have been respectively completed: both achieved satisfactory results.

VI. CONCLUSION

In this paper, for the trajectory tracking control problem of the TianGong-2 manipulator in the floating space of the experimental cabin, a spatial extended state observer is designed to estimate the influence of disturbances, including the gust on the system, and then to the design of rapid capture. A fuzzy control strategy based on a spatial extended state observer is proposed. More specifically, a fuzzy controller based on extended observer is designed to ensure the rapid convergence of the desired trajectory: hence, the Lyapunov function is used to prove the closed-loop stability, and then, the simulation and experimentation of the task of catching floating buoys in space are carried out. Generally, the results show that the FC-SESO controller proposed in this paper exhibits good trajectory tracking performance for quick capture tasks in different gravitational environments.

In the space station environment, uncertainties and disturbances include not only wind gust disturbances but also unknown conditions such as terminal load, friction force, gravitational field, temperature field, and irregular vibration. The influences of these uncertainties on the accuracy of the manipulator can be further discussed in future research.

REFERENCES

[1] J. Parrish, B. Sullivan, and B. Roberts, "Planning for the ranger telerobotic shuttle experiment on-orbit operations," in *Proc. Space Conf. Expo.*, Sep. 2000, p. 5291.

[2] A. Robertson, G. Inalhan, and J. How, "Spacecraft formation flying control design for the Orion mission," in *Proc. Guid., Navigat. Control Conf. Exhibit*, Aug. 1999, p. 4266.

[3] T. Sugimoto, H. Tsunoda, K.-I. Hariu, Y. Kawakami, K. Miyoshi, J. Nakagawa, T. Sugimoto, H. Tsunoda, K.-I. Hariu, Y. Kawakami, K. Miyoshi, and J. Nakagawa, "Structural design and deployment test methods for a large deployable mesh reflector," in *Proc. 38th Struct., Struct. Dyn, Mater. Conf.*, Apr. 1997, p. 1148.

[4] M. Nagatomo, T. Mitome, K. Kawasaki, N. Ezawa, and K. Kasuga, "MFD robot arm and its flight experiment," in *Proc. Space*, Apr. 1998, pp. 319–324.

[5] H. Sawada, K. Ui, M. Mori, H. Yamamoto, R. Hayashi, S. Matunaga, and Y. Ohkami, "Micro-gravity experiment of a space robotic arm using parabolic flight," *Adv. Robot.*, vol. 18, no. 3, pp. 247–267, Jan. 2004.

[6] C. Chang, J. Liu, Z. Ni, and R. Qi, "An improved kinematic calibration method for serial manipulators based on POE formula," *Robotica*, vol. 36, no. 8, pp. 1244–1262, Aug. 2018.

[7] Z. Ni, J. Liu, Z. Wu, and X. Shen, "Identification of the state-space model and payload mass parameter of a flexible space manipulator using a recursive subspace tracking method," *Chin. J. Aeronaut.*, vol. 32, no. 2, pp. 513–530, Feb. 2019.

[8] X. Zhang and J. Liu, "Effective motion planning strategy for space robot capturing targets under consideration of the berth position," *Acta Astronautica*, vol. 148, pp. 403–416, Jul. 2018.

[9] X. Zhang and J. Liu, "Autonomous trajectory planner for space telerobots capturing space debris under the teleprogramming framework," *Adv. Mech. Eng.*, vol. 9, no. 9, Sep. 2017, Art. no. 168781401772329.

[10] P. Ouyang, J. Acob, and V. Pano, "PD with sliding mode control for trajectory tracking of robotic system," *Robot. Comput.-Integr. Manuf.*, vol. 30, no. 2, pp. 189–200, Apr. 2014.

[11] A. Kumar, P. M. Pathak, and N. Sukavanam, "Trajectory control of a two DOF rigid–flexible space robot by a virtual space vehicle," *Robot. Auto. Syst.*, vol. 61, no. 5, pp. 473–482, May 2013.

[12] X. Li and C. C. Cheah, "Global task-space adaptive control of robot," *Automatica*, vol. 49, no. 1, pp. 58–69, Jan. 2013.

[13] M. Sabatini, R. Monti, P. Gasbarri, and G. B. Palmerini, "Adaptive and robust algorithms and tests for visual-based navigation of a space robotic manipulator," *Acta Astronautica*, vol. 83, pp. 65–84, Feb. 2013.

[14] X. Zhao, X. Wang, S. Zhang, and G. Zong, "Adaptive neural backstepping control design for a class of nonsmooth nonlinear systems," *IEEE Trans. Syst., Man, Cybern., Syst.*, vol. 49, no. 9, pp. 1820–1831, Sep. 2019.

[15] H. Wang, P. X. Liu, J. Bao, X.-J. Xie, and S. Li, "Adaptive neural output-feedback decentralized control for large-scale nonlinear systems with stochastic disturbances," *IEEE Trans. Neural Netw. Learn. Syst.*, to be published.

[16] Y. N. Fei, J. S. Smith, and Q. H. Wu, "Sliding mode control of robot manipulators based on sliding mode perturbation observation," *Proc. Inst. Mech. Eng., I, J. Syst. Control Eng.*, vol. 220, no. 3, pp. 201–210, May 2006.

[17] R. Madoński and P. Herman, "Survey on methods of increasing the efficiency of extended state disturbance observers," *ISA Trans.*, vol. 56, pp. 18–27, May 2015.

[18] B. Liu, "Speed control for permanent magnet synchronous motor based on an improved extended state observer," *Adv. Mech. Eng.*, vol. 10, no. 1, Jan. 2018, Art. no. 168781401774766.

[19] S. Xiong, W. Wang, X. Liu, Z. Chen, and S. Wang, "A novel extended state observer," *ISA Trans.*, vol. 58, pp. 309–317, Sep. 2015.

[20] F. Yang, C.-Z. Wei, R. Wu, and N.-G. Cui, "Non-recursive fixed-time convergence observer and extended state observer," *IEEE Access*, vol. 6, pp. 62339–62351, 2018.

[21] R. Cui, L. Chen, C. Yang, and M. Chen, "Extended state observer-based integral sliding mode control for an underwater robot with unknown disturbances and uncertain nonlinearities," *IEEE Trans. Ind. Electron.*, vol. 64, no. 8, pp. 6785–6795, Aug. 2017.

[22] S. Xingling and W. Honglun, "Trajectory linearization control based output tracking method for nonlinear uncertain system using linear extended state observer," *Asian J. Control*, vol. 18, no. 1, pp. 316–327, Jan. 2016.

[23] H. Pan, W. Sun, H. Gao, T. Hayat, and F. Alsaadi, "Nonlinear tracking control based on extended state observer for vehicle active suspensions with performance constraints," *Mechatronics*, vol. 30, pp. 363–370, Sep. 2015.

[24] Q. Chen, Y.-R. Nan, H.-H. Zheng, and X.-M. Ren, "Full-order sliding mode control of uncertain chaos in a permanent magnet synchronous motor based on a fuzzy extended state observer," *Chin. Phys. B*, vol. 24, no. 11, Nov. 2015, Art. no. 110504.

[25] J. Qian, A. Xiong, and W. Ma, "Extended state observer-based sliding mode control with new reaching law for PMSM speed control," *Math. Problems Eng.*, vol. 2016, Jun. 2016, Art. no. 6058981.

[26] F. Zhang, X. Wu, and J. Shen, "Extended state observer based fuzzy model predictive control for ultra-supercritical boiler-turbine unit," *Appl. Therm. Eng.*, vol. 118, pp. 90–100, May 2017.

[27] M. Yue, C. An, and Z. Li, "Constrained adaptive robust trajectory tracking for WIP vehicles using model predictive control and extended state observer," *IEEE Trans. Syst., Man, Cybern., Syst.*, vol. 48, no. 5, pp. 733–742, May 2018.

[28] D. Zhai, L. An, J. Dong, and Q. Zhang, "Switched adaptive fuzzy tracking control for a class of switched nonlinear systems under arbitrary switching," *IEEE Trans. Fuzzy Syst.*, vol. 26, no. 2, pp. 585–597, Apr. 2018.

[29] W. Zhang, X. Dong, and X. Liu, "Switched fuzzy-PD control of contact forces in robotic microbiomanipulation," *IEEE Trans. Biomed. Eng.*, vol. 64, no. 5, pp. 1169–1177, May 2017.

[30] R. Sakthivel, S. Harshavarthini, R. Kavikumar, and Y.-K. Ma, "Robust tracking control for fuzzy Markovian jump systems with time-varying delay and disturbances," *IEEE Access*, vol. 6, pp. 66861–66869, 2018.

[31] J. Guan, C.-M. Lin, G.-L. Ji, L.-W. Qian, and Y.-M. Zheng, "Robust adaptive tracking control for manipulators based on a TSK fuzzy cerebellar model articulation controller," *IEEE Access*, vol. 6, pp. 1670–1679, 2018.

[32] H. Navvabi and A. Markazi, "Position control of stewart manipulator using a new extended adaptive fuzzy sliding mode controller and observer (E-AFSMCO)," *J. Franklin Inst.*, vol. 355, no. 5, pp. 2583–2609, Mar. 2018.

[33] Y. Li, S. Tong, and T. Li, "Observer-based adaptive fuzzy tracking control of MIMO stochastic nonlinear systems with unknown control directions and unknown dead zones," *IEEE Trans. Fuzzy Syst.*, vol. 23, no. 4, pp. 1228–1241, Aug. 2015.

[34] F. Yacef, O. Bouhali, M. Hamerlain, and N. Rizoug, "Observer-based adaptive fuzzy backstepping tracking control of quadrotor unmanned aerial vehicle powered by Li-ion battery," *J. Intell. Robot. Syst.*, vol. 84, nos. 1–4, pp. 179–197, Dec. 2016.

[35] H. Chaoui and H. Gualous, "Adaptive fuzzy logic control for a class of unknown nonlinear dynamic systems with guaranteed stability," *J. Control Autom. Electr. Syst.*, vol. 28, no. 6, pp. 727–736, Dec. 2017.

[36] X. Zhao, X. Wang, L. Ma, and G. Zong, "Fuzzy-approximation-based asymptotic tracking control for a class of uncertain switched nonlinear systems," *IEEE Trans. Fuzzy Syst.*, to be published.

[37] P. S. Londhe and B. M. Patre, "Adaptive fuzzy sliding mode control for robust trajectory tracking control of an autonomous underwater vehicle," *Intell. Service Robot.*, vol. 12, no. 1, pp. 87–102, Jan. 2019.

[38] B. Patre, P. Londhe, L. Waghmare, and S. Mohan, "Disturbance estimator based non-singular fast fuzzy terminal sliding mode control of an autonomous underwater vehicle," *Ocean Eng.*, vol. 159, pp. 372–387, Jul. 2018.

[39] S. Waslander and C. Wang, "Wind disturbance estimation and rejection for quadrotor position control," in *Proc. AIAA Infotech Aerosp. Conf.*, Apr. 2009, p. 1983.

[40] D. J. Moorhouse and R. J. Woodcock, "Background information and user guide for Mil-F-8785c, military specification-flying qualities of piloted airplanes," Air Force Wright Aeronaut. Lab., Wright-Patterson AFB, OH, USA, Tech. Rep. AFWAL-TR-81-3109, 1982.

[41] J. Etele and G. Fusina, *Overview of Wind Gust Modelling With Application to Autonomous Low-Level UAV Control*. Toronto, ON, Canada: Defence R&D Canada, 2006.

[42] Y.-M. Chen, Y.-L. He, and M.-F. Zhou, "Decentralized PID neural network control for a quadrotor helicopter subjected to wind disturbance," *J. Central South Univ.*, vol. 22, no. 1, pp. 168–179, Jan. 2015.

[43] D. Shi, Z. Wu, and W. Chou, "Generalized extended state observer based high precision attitude control of quadrotor vehicles subject to wind disturbance," *IEEE Access*, vol. 6, pp. 32349–32359, 2018.

[44] Q. Zheng, L. Q. Gaol, and Z. Gao, "On stability analysis of active disturbance rejection control for nonlinear time-varying plants with unknown dynamics," in *Proc. 46th IEEE Conf. Decis. Control*, Dec. 2007, pp. 3501–3506.

[45] P. Hou, Y. Liu, Z. Xie, and H. Liu, "Development of a space arm-hand system for on-orbit servicing," in *Proc. IEEE Int. Conf. Mechtron. Autom. (ICMA)*, Aug. 2015, pp. 1519–1524.

[46] C. Yu, Z. Li, and H. Liu, "Research on gravity compensation of robot arm based on model learning," in *Proc. IEEE/ASME Int. Conf. Adv. Intell. Mechtron. (AIM)*, Jul. 2019, pp. 635–641.

CHUNGUANG FAN received the B.S. and M.S. degrees in mechanical and power engineering from the Harbin University of Science and Technology (HUST), Harbin, China, in 2009 and 2012, respectively, where he is currently pursuing the Ph.D. degree with the State Key Laboratory of Robotics and System. His research interests include space manipulators, space microgravity, and human robot interaction.

ZONGWU XIE received the B.S. degree in mechanical and power engineering from the Harbin University of Science and Technology (HUST), Harbin, China, in 1996, and the M.S. and Ph.D. degrees in mechatronics engineering from the Harbin Institute of Technology (HIT), Harbin, in 2000 and 2003, respectively, where he is currently an Associate Professor and a Ph.D. Supervisor with the School of Mechatronics Engineering. His research interests include space robots and drive and control of robots.

YIWEI LIU received the M.S. and Ph.D. degrees in mechatronics engineering from the Harbin Institute of Technology (HIT), Harbin, China, in 2002 and 2006, respectively, where he is currently an Associate Professor and a Ph.D. Supervisor with the School of Mechatronics Engineering. His research interests include space robots, structural design, and sensor design.

CHONGYANG LI received the B.S. degree in mechanical and electrical engineering from the Huazhong University of Science and Technology (HUST), Wuhan, China, in 2013, and the M.S. degree in mechatronics engineering from the Harbin Institute of Technology (HIT), Harbin, China, in 2015, where he is currently pursuing the Ph.D. degree with the State Key Laboratory of Robotics and System. His research interests include space manipulators, learning from demonstration, optimal control, and human robot interaction.

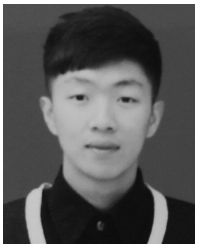

CHENGLONG YU received the B.S. degree in mechanical and power engineering from Harbin Engineering University (HEU), Harbin, China, in 2015, and the M.S. degree in mechanical and power engineering from the Harbin University of Science and Technology (HUST), Harbin, in 2017, where he is currently pursuing the Ph.D. degree with the State Key Laboratory of Robotics and System. His research interests include space manipulators, robot simulation, and human robot interaction.

HONG LIU received the Ph.D. degree from the Harbin Institute of Technology (HIT), China, in 1993. From 1991 to 1993, he was a joint Ph.D. candidate with the Institute of Robotics and System Dynamics, German Aerospace Research Establishment (DLR), Germany, where he had been a Research Fellow, since 1993. He became one of the first Changjiang Scholars, in 1998. He is currently a Professor with HIT. His research projects include the development of dexterous robot hands and space manipulators.